Inverting RANSAC: Global Model Detection via Inlier Rate Estimation

– Supplementary materials–

Contents

A. Proof that $d_{\max}(p)$ Attains a Local Minimum at $p = p^\star$

The standard way of showing that a C^1 function attains its minimum at a point is by showing a vanishing first-order derivative at that point, in our case, $\frac{\partial d_{\max}}{\partial p}\big|_{p=p^\star}$. However, as we show below, $d_{\max}(p)$ is not differentiable at $p = p^\star$; we will therefore show that the left and right derivatives of $d_{\max}(p)$ at $p^\star$ are, respectively, negative and positive. We obtain the derivative $\frac{\partial d_{\max}(p)}{\partial p}$ by using the equation

$$
\begin{aligned}
p \;=\; & \rho_{\text{in}} \cdot \psi(r^\star, r_{\min}(p)+\delta, d_{\max}(p)) \cdot p^\star + ... \\
& \rho_{\text{out}} \cdot \left(\pi \cdot (r_{\min}(p)+\delta)^2 - \psi(r^\star, r_{\min}(p)+\delta, d_{\max}(p))\right) \cdot (1-p^\star),
\end{aligned}
\tag{A.1}
$$

which was obtained by plugging $p_t(r_{\min}(p)+\delta) = p$ from inequality (13) into equation (15). This can be rewritten as the simplified expression

$$
\psi(r^\star, r_{\min}(p)+\delta, d_{\max}(p)) = \frac{p - \pi(r_{\min}(p) + \delta)^2(1-p^\star) \cdot \rho_{\text{out}}}{p^\star \cdot \rho_{\text{in}} - (1-p^\star) \cdot \rho_{\text{out}}} \triangleq G(p).
$$

Since ψ is not easily invertible (see (A.7) below), we define the implicit equation $F(p, d_{\max}(p)) = 0$ with

$$
F(p, d) = \psi(r^\star, r_{\min}(p)+\delta, d) - G(p)
\tag{A.2}
$$

and use implicit differentiation

$$
\frac{\partial d_{\max}(p)}{\partial p} = -\frac{\partial F/\partial p}{\partial F/\partial d_{\max}(p)}.
\tag{A.3}
$$

A.1. Calculating $r_{\min}(p)$

Under the assumption of uniform f_{in} and f_{out}, we further assume

$$
\rho_{\text{in}} \cdot p^\star > \rho_{\text{out}} \cdot (1 - p^\star)
\tag{A.4}
$$

(otherwise there is a transformation more prominent than $t^\star$). The best attainable error $r_{\min}(p)$ can now the value of can be directly computed, and shown to be

$$r_{\min}(p) = \begin{cases} r^\star \cdot \sqrt{p/p^\star} & p \leq p^\star \\ \sqrt{\frac{p-p^\star}{\pi \rho_{\mathrm{out}}} + r^{\star 2}} & p \geq p^\star \end{cases} \tag{A.5}$$

Note that the two cases $p \leq p^\star$ and $p \geq p^\star$ coincide at $p = p^\star$, sharing the value $r_{\min}(p^\star) = r^\star$ (obtained, e.g., by the transformation $t^\star$). TODO: Add a simple explanatory illustration for both the cases. Let us look at each of the two cases:

The case $p \geq p^\star$ here we have $r^\star < r_{\min}(p)$, and following A.4 we get that $\mathrm{B}_{r^\star}(t^\star) \subset \mathrm{B}_{r_{\min}(p)}(t)$ for any transformation t that obtains $r_{\min}(p)$. As $r_{\min}(p)$ is rather larger than $r^\star$, its size depends on the distribution ρ_{out}, resulting in $\rho_{\mathrm{out}} \cdot (\pi r_{\min}(p)^2 - \pi r^{\star 2}) = p - p^\star$. We can then extract

$$r_{\min}(p) = \sqrt{\frac{p - p^\star}{\rho_{\mathrm{out}}\pi} + r^{\star 2}} \tag{A.6}$$

The case $p < p^\star$ In this case p is an underestimate of $p^\star$ and therefore $r_{\min}(p) < r^\star$, and similarly $\mathrm{B}_{r^\star}(t^\star) \supset \mathrm{B}_{r_{\min}(p)}(t)$. Since $p/p^\star = \pi r_{\min}(p)^2 / \pi r^{\star 2}$, we obtain in this case that $r_{\min}(p) = r^\star \cdot \sqrt{p/p^\star}$.

A.2. The function ψ

ψ returns the intersection area of two circles with radii r_1 and r_2, whose centers are d apart. The range of interest is $|r_1 - r_2| < d < r_1 + r_2$, out of which there is either full or empty intersection. The formula for ψ was taken from equation (14) in [2].

$$\psi(r_1, r_2, d) = r_1^2 \cos^{-1}\left(\frac{d^2 + r_1^2 - r_2^2}{2dr_1}\right) + r_2^2 \cos^{-1}\left(\frac{d^2 - r_1^2 + r_2^2}{2dr_2}\right) \tag{A.7}$$
$$- \frac{\sqrt{(d + r_1 - r_2)(d - r_1 + r_2)(r_1 - d + r_2)(d + r_1 + r_2)}}{2}$$

The partial derivatives of ψ, w.r.t. d as well as r_1 (and r_2 similarly) are

$$\frac{\partial \psi(r_1, r_2, d)}{\partial d} = -\frac{1}{d}\sqrt{(d + r_1 - r_2)(d - r_1 + r_2)(r_1 - d + r_2)(d + r_1 + r_2)} \tag{A.8}$$

$$\frac{\partial \psi(r_1, r_2, d)}{\partial r_1} = 2r_1 \cos^{-1}\left(\frac{d^2 + r_1^2 - r_2^2}{2dr_1}\right) \tag{A.9}$$

A.3. Derivatives of $F(p, d_{\max}(p))$

The derivative w.r.t. $d_{\max}(p)$ given by

$$\frac{\partial F}{\partial d_{\max}(p)} = \frac{\partial \psi}{\partial d}\Big|_{d = d_{\max}(p)} \tag{A.10}$$

is always negative, as the derivative $\frac{\partial \psi}{\partial d}$ is always negative (since the circles intersection areas decreases as d increases). Next, to get the derivative w.r.t. p we first derive $r_{\min}(p)$

$$\frac{\partial r_{\min}(p)}{\partial p} = \begin{cases} \frac{r^\star}{2p^\star \sqrt{\frac{p}{p^\star}}} & p \leq p^\star \\ \left(2\pi\rho_{\mathrm{out}}\sqrt{r^{\star 2} + \frac{p-p^\star}{\pi\rho_{\mathrm{out}}}}\right)^{-1} & p \geq p^\star \end{cases} \xrightarrow{p \to p^\star} \begin{cases} r^\star/2p^\star \\ (2\pi\rho_{\mathrm{out}}r^\star)^{-1} \end{cases} \tag{A.11}$$
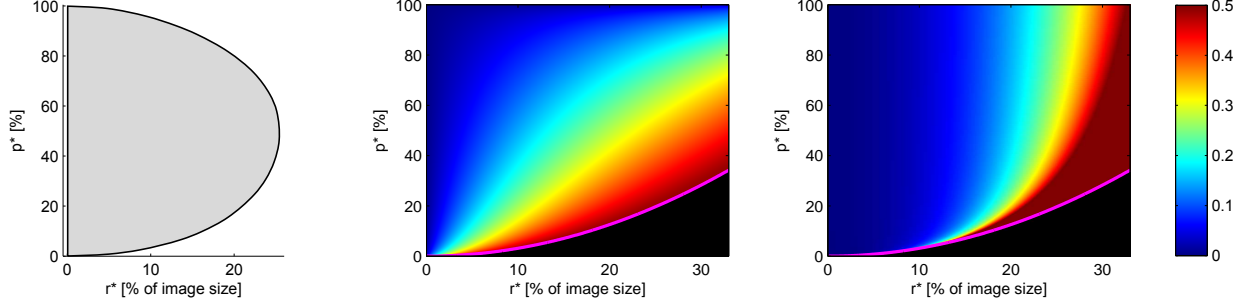
Figure A.1: **Visual analysis of** (A.18) **for** $\delta \to 0$. Left: the region where (A.18) holds, and therefore $d_{\max}(p)$ attains a local minimum (identical to Figure 4 in the paper). Center and Right: color-mapped values of the left and right hand sides of (A.18), accordingly. The black regions under the curve $p^\star = \pi \cdot r^{\star 2}$ (in magenta), are locations where the left hand side of (A.18) is undefined.

then we derive $G(p)$

$$
\frac{\partial G}{\partial p} = \begin{cases} \dfrac{\frac{\pi \rho_{\text{out}} r^\star \left(\delta + r^\star \sqrt{\frac{p}{p^\star}}\right)(p^\star - 1)}{p^\star \sqrt{\frac{p}{p^\star}}} + 1}{p^\star \cdot \rho_{\text{in}} - (1 - p^\star) \cdot \rho_{\text{out}}} & p \leq p^\star \\[4ex] \dfrac{\frac{\left(\delta + \sqrt{r^{\star 2} + \frac{p - p^\star}{\pi \rho_{\text{out}}}}\right)(p^\star - 1)}{\sqrt{r^{\star 2} + \frac{p - p^\star}{\pi \rho_{\text{out}}}}} + 1}{p^\star \cdot \rho_{\text{in}} - (1 - p^\star) \cdot \rho_{\text{out}}} & p \geq p^\star \end{cases} \xrightarrow{p \to p^\star} \begin{cases} \dfrac{\frac{\pi \rho_{\text{out}} r^\star (\delta + r^\star)(p^\star - 1)}{p^\star} + 1}{p^\star \cdot \rho_{\text{in}} - (1 - p^\star) \cdot \rho_{\text{out}}} \\[4ex] \dfrac{\frac{(\delta + r^\star)(p^\star - 1)}{r^\star} + 1}{p^\star \cdot \rho_{\text{in}} - (1 - p^\star) \cdot \rho_{\text{out}}} \end{cases} \tag{A.12}
$$

and finally the function F

$$
\frac{\partial F}{\partial p} = \left. \frac{\partial \psi}{\partial r_1} \right|_{r_1 = (r_{\min}(p) + \delta)} \cdot \frac{\partial r_{\min}(p)}{\partial p} - \frac{\partial G}{\partial p}. \tag{A.13}
$$

Plugging (A.11) and (A.12) into (A.13) we get

$$
\left. \frac{\partial F}{\partial p} \right|_{p = p^{\star -}} = \cos^{-1}\left(\frac{d_{\max}(p)^2 + \delta^2 + 2r^\star \delta}{2 d_{\max}(p) (\delta + r^\star)} \right) \frac{r^\star (\delta + r^\star)}{p^\star} - \frac{\pi \rho_{\text{out}} r^\star (\delta + r^\star)(p^\star - 1) + p^\star}{p^\star (p^\star \cdot \rho_{\text{in}} - (1 - p^\star) \cdot \rho_{\text{out}})} \tag{A.14}
$$

$$
\left. \frac{\partial F}{\partial p} \right|_{p = p^{\star +}} = \cos^{-1}\left(\frac{d_{\max}(p)^2 + \delta^2 + 2\delta r^\star}{2 d_{\max}(p) (\delta + r^\star)} \right) \frac{(\delta + r^\star)}{\pi \rho_{\text{out}} r^\star} - \frac{(p^\star - 1)(\delta + r^\star) + r^\star}{r^\star (p^\star \cdot \rho_{\text{in}} - (1 - p^\star) \cdot \rho_{\text{out}})} \tag{A.15}
$$

A.4. Ranges where the solution is valid

For the minimum to exist, we need to show that $\frac{\partial F}{\partial p}$ is positive for $p \geq p^\star$ and negative for $p \leq p^\star$, .i.e.

$$
\left. \frac{\partial F}{\partial p} \right|_{p = p^{\star -}} < 0 \qquad \text{and} \qquad \left. \frac{\partial F}{\partial p} \right|_{p = p^{\star +}} > 0 \tag{A.16}
$$

After plugging in the values of ρ_{in} and ρ_{out} into (A.14) and (A.15) and some simplifications, we respectively obtain

$$
\frac{1}{\pi} \cos^{-1}\left(\frac{d_{\max}(p)^2 + \delta^2 + 2r^\star \delta}{2 d_{\max}(p) (\delta + r^\star)} \right) < \frac{r^\star \left(p^\star - \pi r^{\star 2} - \pi \delta r^\star + \pi \delta p^\star r^\star\right)}{(\delta + r^\star)\left(p^\star - \pi r^{\star 2}\right)} \tag{A.17}
$$

$$
\frac{1}{\pi} \cos^{-1}\left(\frac{d_{\max}(p)^2 + \delta^2 + 2\delta r^\star}{2 d_{\max}(p) (\delta + r^\star)} \right) > \frac{\pi r^{\star 2} \left(\delta p^\star - \delta + p^\star r^\star\right)}{(\delta + r^\star)\left(p^\star - \pi r^{\star 2}\right)} \tag{A.18}
$$

Let us examine the case of $\delta \to 0$, where the condition (A.17) always holds as the righthand side approaches 1, which is always larger than $\cos^{-1}$ (upper bounded by $\pi/2$ for positive input). The condition in (A.18) is a little more subtle, and Figure A.1 shows its left and right hand sides, for $\delta \to 0$. The regions in Figure 4 in the paper originate form this analysis.

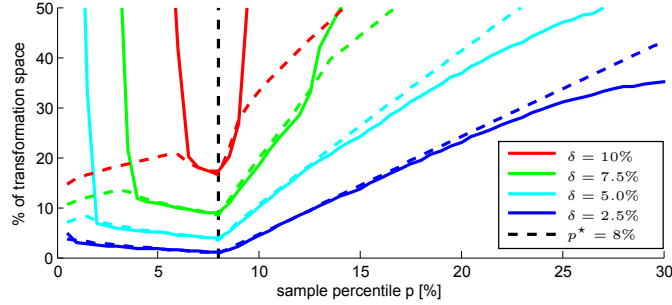Figure B.2: **This is a replica of Figure 6 from the paper.**

B. Discussion on the Interval where Theoretical and Empirical Curves Match (Figure 6)

As can be seen in Figure 6 in the paper (also shown as Figure B.2 here), there is an evident match between theory and practice at a certain interval around the true inlier rate $p^\star$, but the extent of this interval diminishes with the increase in δ. As done above in Section A.1 for $r_{\min}(p)$, we split the discussion into two cases:

The case $p < p^\star$: As p decreases below a certain value which we denote by p_1, a disk of radius $r_{\min}(p) + \delta$ can have a probability of p even if it does not intersect $\mathrm{B}_{r^*}(T^*)$. Therefore, beyond the point p_1 the value $V_\delta(p)$ will increase faster than the theoretic curve, and $\Omega_\delta(p)$ gradually captures the whole space $\mathcal{T}$.

The value of p_1 can be roughly calculated. Once again, assuming uniform outlier density ρ_{out}, we obtain that $p_1 = \rho_{\mathrm{out}} \cdot \pi \cdot (r_{\min}(p) + \delta)^2$, meaning that p_1 grows with δ, as can be observed in the figure. We did not model this fact in our formulation therefore it happens only in the empirical plot and not in the theoretic one.

The case $p > p^\star$: This case is slightly more involved compared to the previous. At large, it happens due to boundary effects, where the circles that we analyze exceed the image boundaries. Specifically, there are two different deviations from the theoretical analysis. First, as p increases, more of the disks of radius $r_{\min}(p) + \delta$ will capture areas that exceed the boundaries of I_2, and in these areas the match probability density is zero. Hence, the probability that they capture will not grow with p as expected, and therefore less transformations will belong to $\Omega_\delta(p)$. This effect happens earlier for larger δ, as the radii $r_{\min}(p) + \delta$ are larger.

Second, a similar effect happens specifically to balls around $T^*(q_1)$. As p grows, once these balls exceed the boundaries of I_2, the best error $r_{\min}(p)$ might be obtained by transformations other than $t^\star$, especially ones that map points to a more central area of I_2. Moreover, for large enough values of δ, as p grows the balls of radius $r_{\min}(p) + \delta$ capture the entire distribution (which is limited to the image bounds) and $\Omega_\delta(p)$ gradually captures the whole space $\mathcal{T}$ (as can be seen e.g. in the red curve).

C. Additional 2D-Homography Examples (for experiment of Section 4.3)

In this section we present visualizations similar to Figure 8 in the paper, that accompany the 2D-Homography results we report in table 1. Figures C.3, C.4 and C.5 show results on pairs 1–4, 1–5 and 1–6 respectively, which are the three most difficult image pairs from each of the sequences in [1].

References

[1] K. Mikolajczyk and C. Schmid. A performance evaluation of local descriptors. *Pattern Analysis and Machine Intelligence, IEEE Transactions on*, 27(10):1615–1630, 2005. 4, 5, 6, 7

[2] E. W. Weisstein. "circle-circle intersection" from mathworld. http://mathworld.wolfram.com/Circle-CircleIntersection.html, 2014. [Online; accessed 21-July-2014]. 2
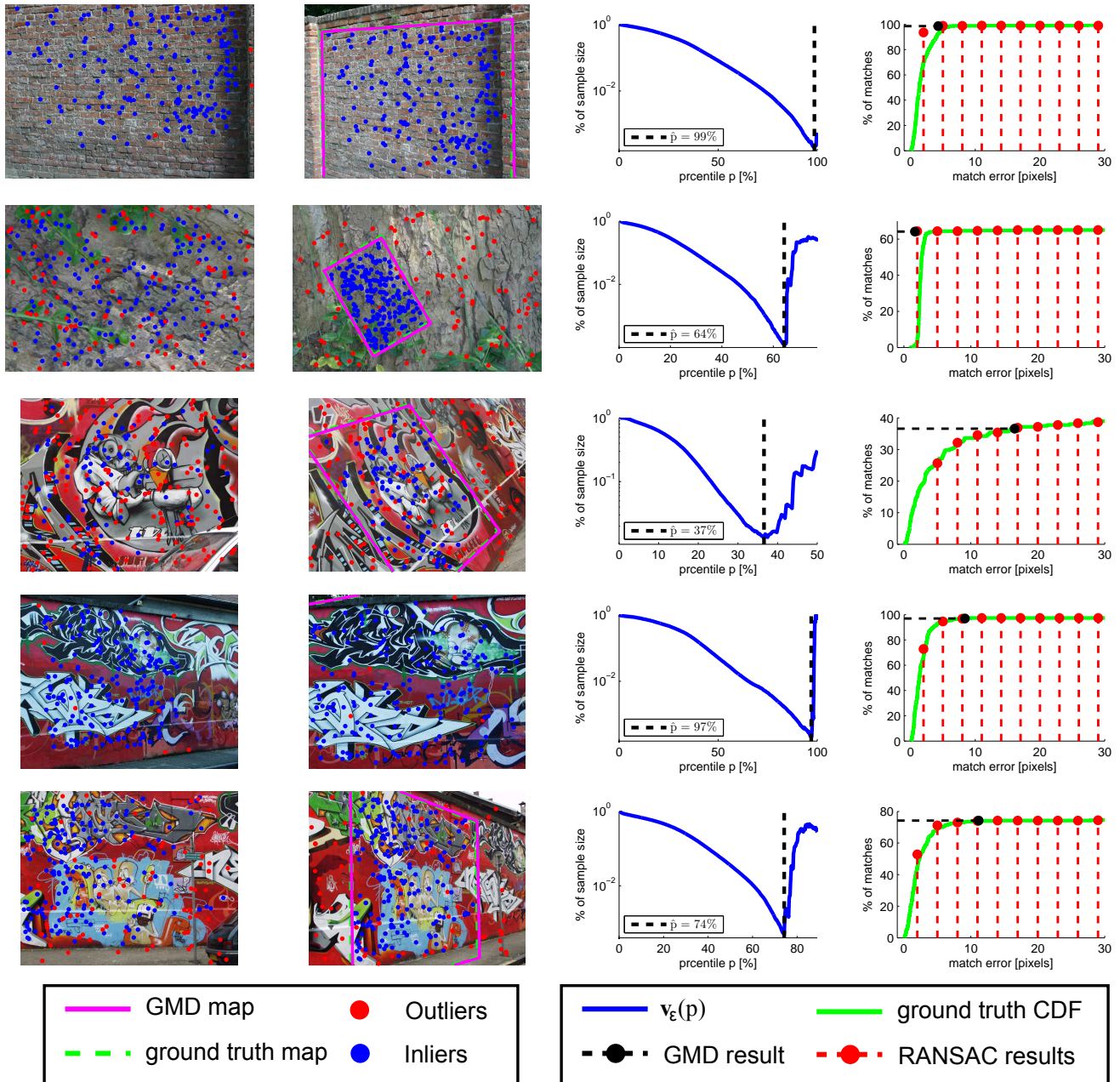
Figure C.3: **Results for Frames 1-4 on five sequences from [1].** Sequence names from top to bottom are: 'wall', 'bark', 'graffiti', 'graffiti 4' and 'graffiti 5'. In each row from the left: **Image** I_1 with inliers (blue) and outliers(red) ; **Image** I_2 like the former, along with the ground-truth and GMD map of I_1 (green and magenta, respectivley); **IRE prediction** $\hat{p}$ (black dashed line) as the minimal value of $\mathbf{v}_\varepsilon(p)$ (blue, log-scale axis) ; **Final results**: The result of GMD (black circle) and the result of multiple USAC runs for different thresholds (red circles), shown against the CDF (green curve) of match-errors w.r.t. the ground-truth transformation. Missing red line means failed USAC runs.
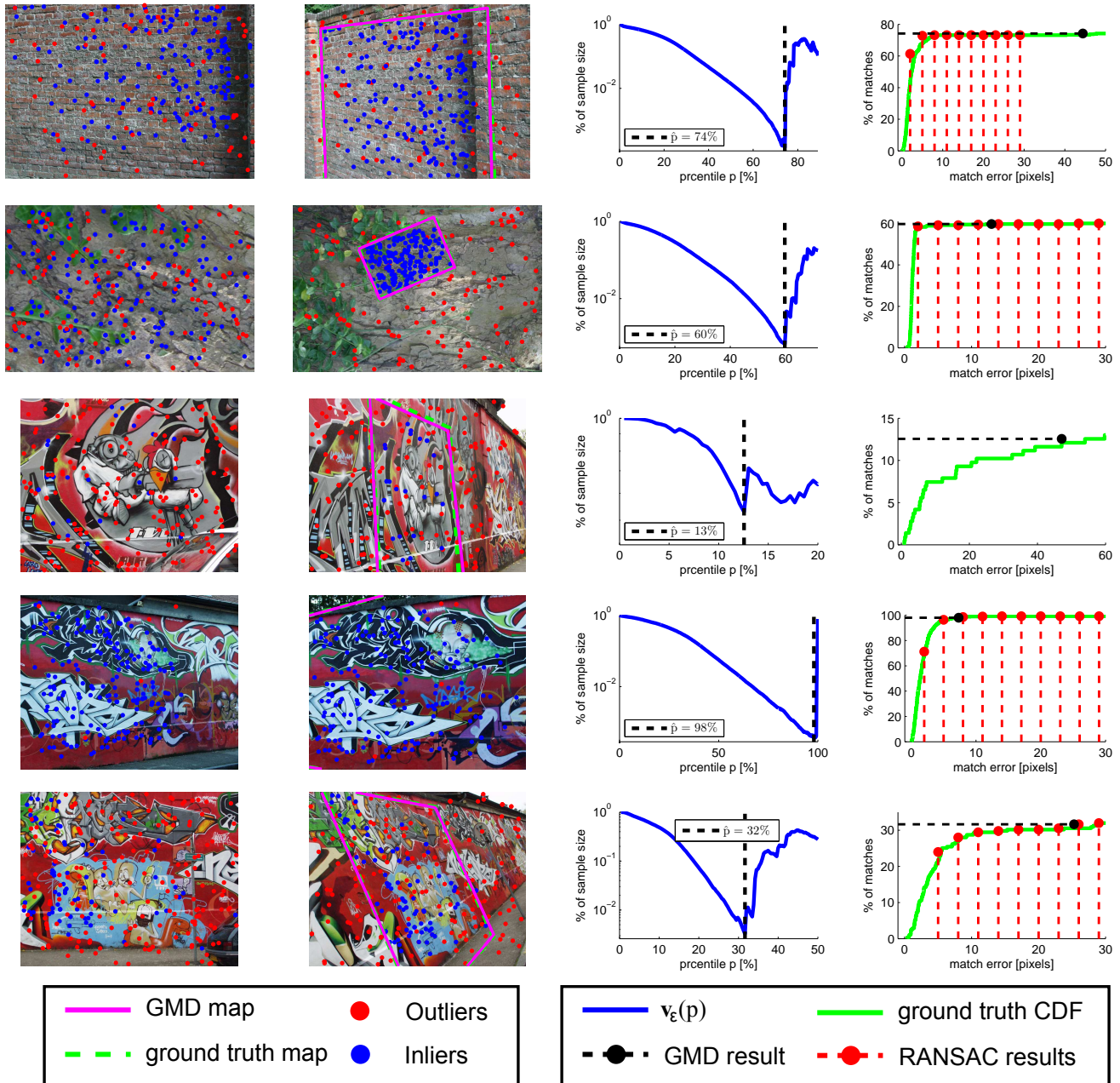
Figure C.4: **Results for Frames 1-5 on five sequences from [1].** Sequence names from top to bottom are: 'wall', 'bark', 'graffiti', 'graffiti 4' and 'graffiti 5'. In each row from the left: **Image** I_1 with inliers (blue) and outliers(red) ; **Image** I_2 like the former, along with the ground-truth and GMD map of I_1 (green and magenta, respectivley); **IRE prediction** $\hat{p}$ (black dashed line) as the minimal value of $\mathbf{v}_\varepsilon(p)$ (blue, log-scale axis) ; **Final results**: The result of GMD (black circle) and the result of multiple USAC runs for different thresholds (red circles), shown against the CDF (green curve) of match-errors w.r.t. the ground-truth transformation. Missing red line means failed USAC runs.
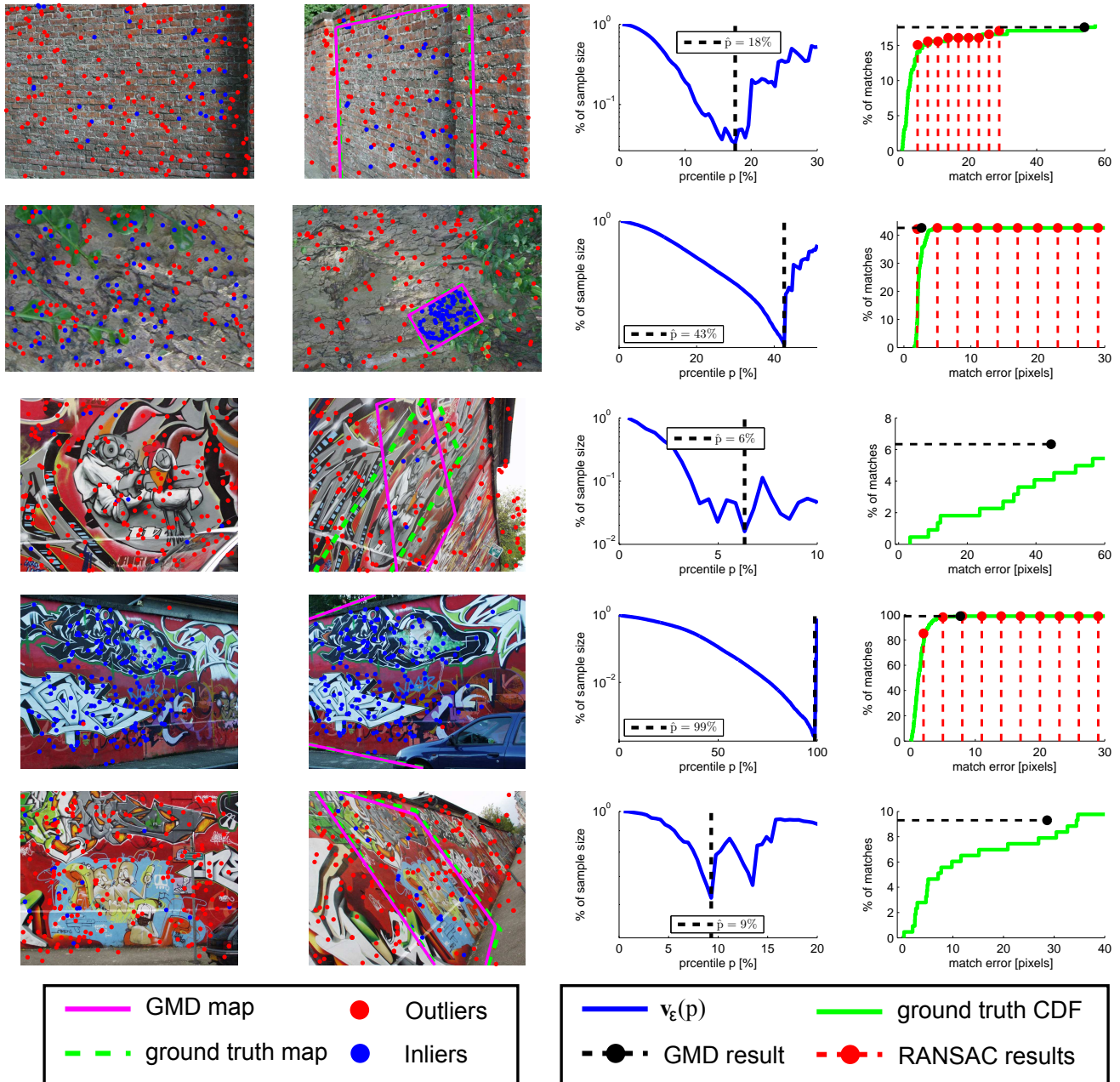
Figure C.5: **Results for Frames 1-6 on five sequences from [1].** Sequence names from top to bottom are: 'wall', 'bark', 'graffiti', 'graffiti 4' and 'graffiti 5'. In each row from the left: **Image** I_1 with inliers (blue) and outliers(red) ; **Image** I_2 like the former, along with the ground-truth and GMD map of I_1 (green and magenta, respectivley); **IRE prediction** $\hat{p}$ (black dashed line) as the minimal value of $\mathbf{v}_\varepsilon(p)$ (blue, log-scale axis) ; **Final results**: The result of GMD (black circle) and the result of multiple USAC runs for different thresholds (red circles), shown against the CDF (green curve) of match-errors w.r.t. the ground-truth transformation. Missing red line means failed USAC runs.